ACKNOWLEDGEMENT

The authors wish to acknowledge the support and assistance of J. C. Swearengen, 8436, who provided the original impetus for this work. The reviewers of this report, M. L. Chiesa, 8241 and N. A. Lapetina, 8436, are also acknowledged for their thoughtful suggestions and careful reading of the rough draft. The HULL calculations described in this report were carried out by P. Yarrington, 1533.

Table of Contents

Introduction 15

1 Preliminary Considerations 16

1.1 Penetrator Properties 16

1.2 Rubble Properties 17

2 Penetrator Equations of Motion 17

2.1 Assumptions and Limitations 18

2.2 Solving for the Impact Angle, γ 20

2.3 Solving for Velocity Angle, β, and Angle of Attack, α 22

3 Parametric Study of the Penetrator Equations of Motion 22

3.1 Initial Angle of Attack, α_1 23

3.2 Initial Impact Angle, γ_1 24

3.3 Contact Angle, θ 24

3.4 Height at Point of Contact, H 27

3.5 Force Between the Boulder and the Penetrator, F 28

3.6 Initial Velocity of the Penetrator, v_1 29

3.7 Penetrator Mass Properties, m, I_{cg} 32

3.8 Summary 35

3.8.1 Overview of the Effects of Parameter Variations 39

3.8.2 Final Impact Angle, γ_3 40

3.8.3 Final Angle of Attack, α_3 40

4 Series of Impacts 41

5 Lateral Loads Induced on Target Entry 42

6 Conclusions 46

References 47

Illustrations

No. Page

1. Definition of EPW Dimensions for Table 1. 16

2. Example of EPW Encounters with Various Obstacles. 17

3. Free Body Diagrams of the EPW and Obstacle. 18

4. The Angle of Attack, α, Impact Angle, γ, Velocity Vector Angle, β, and the Nose Angle, ϕ. 19

5. Effect of Reduced Moment Arm and Lateral Load Due to a Smaller Area of Contact 20

6.

7.

8.

9.

10.

11.

12.

13.

14.

15.

16.

17.

DOD
MCTL
b(3)

18.

19.

20.

21.

22.

23.

24.

26.

25.

DCD 27.

MCTL 28.

b(3)

29.

30.

31.

32.

34.

33.

35.

36.

Tables

No. Page

1. Penetrator Properties 16

2. Varying α_1 for EPW-1 23

3. Trends Identified by Parametric Study of Equations of Motion 40

4. Series of Impacts - Example 1 41

5. Series of Impacts - Example 2 42

6. Series of Impacts - Example 3 42

Effect of Above-Ground Oblique Impacts on the Performance of an Earth Penetrator

Introduction

Analyses of proposed impact scenarios suggest there is a reasonable probability that an earth penetrator will strike an obstacle before hitting the ground. Examples of potential obstacles include urban rubble (e.g., buildings and concrete slabs), boulders, and trees. Encounters with these obstructions could induce lateral impulses large enough to change the trajectory of the penetrator. Other workers have studied various aspects of this problem both analytically and experimentally. For example, Nelson et al.

DOD NCTL (3)

To our knowledge, however, no closed-form solution based on first principles has been developed to treat problems of this type. Such a technique offers the advantage of simple implementation and rapid solution times compared to the computer-intensive numerical techniques that have been employed by other workers. Some of the computational methods that have been used include: CALSAP [2], an implicit finite element code; PROBS [2], an explicit time integration scheme; HULL, a 3-D finite element, Lagrangian/Eulerian, code [5]; and TRIFLE a quasi 3-D finite element code [6]. While these techniques provide useful solutions for a limited number of specialized problems, their complexity make it difficult to examine how these solutions might be affected by realistic parameter variations. For this reason, there is a need for a simplified, closed-form solution technique for problems of this type.

DOD NCTL (5)

* Caliber is defined as the ratio of boulder diameter to penetrator diameter.

1. Preliminary Considerations

1.1. Penetrator Properties

Four penetrator designs were considered in this study (see Table 1).

DOD
MCTL
b(3)

The parameters in Table 1 are defined in Figure 1. Since EPW designs are currently evolving, the results presented in the remainder of this report should only be used by the reader to suggest general trends rather than as precise numbers appropriate for a final EPW design.

DOD
MCTL
b(3)

its velocity vector.) For this reason, our efforts have focused on developing a solution for this angle. Obtaining this solution, however, first requires the derivation of expressions for two other angles: the impact angle, γ and the velocity vector angle, β. γ is defined as the angle between the horizontal axis of the nonrotating reference frame and the EPW's axis (positive clockwise), while β is defined as the angle between the penetrator's velocity vector and the horizontal axis (positive clockwise). The relationship between these angles is shown in Figure 4. The formulations for β and γ are derived first which then are used to solve for α from the geometric relation, $\beta = \alpha + \gamma$.

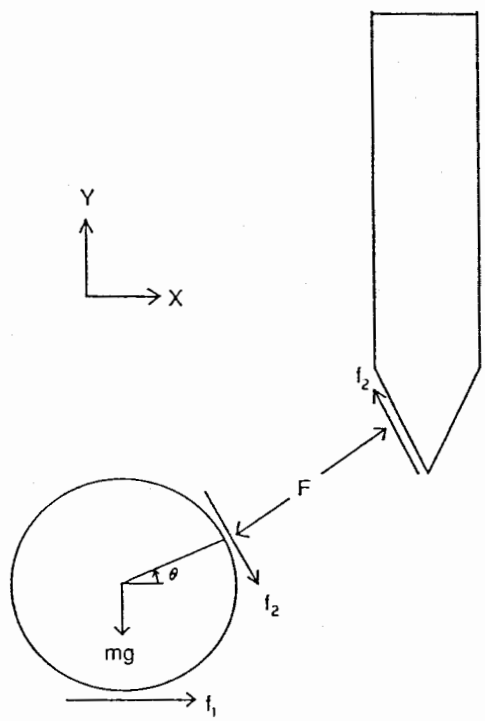

Figure 3. Free Body Diagrams of the EPW and Obstacle.

Three geometric points are especially important in the development of the solution: Point 1, where the EPW contacts the boulder; Point 2, where the EPW leaves the boulder; and Point 3, where the EPW strikes the ground. Labels for these points are used as parameter subscripts to identify relevant aspects of the solution.

2.1. Assumptions and Limitations

An explicit understanding of the assumptions involved in the derivation of the equations of motion is crucial to interpreting the results. As stated above, the first assumption is that the EPW and boulder experience only rigid body, planar motion. We also assume that the force, F, (see Figure 3) is constant while the penetrator is in contact with the boulder. (Additional aspects of this force definition are discussed in section 3.5.) Other assumptions are that the initial angular velocities ($\dot{\alpha}_1$ and $\dot{\gamma}_1$) of the penetrator are zero,

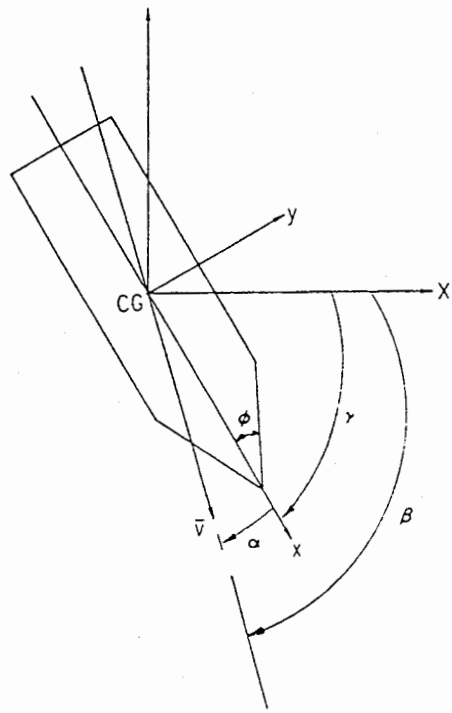

Figure 4. The Angle of Attack, α, Impact Angle, γ, Velocity Vector Angle, β, and the Nose Angle, ϕ.

and the time of contact between the penetrator and the boulder, t_{12}, is given by the EPW nose cone length, L_n, divided by the impact velocity.

The development of the equations of motion can be further simplified by assuming that the position of the boulder is fixed. That is, the boulder does not roll or slide under the action of F. This assumption can be readily justified for relatively massive boulders and high-velocity encounters. For example, a 4-foot diameter boulder would be expected to weigh on the order of 5500 lbs. This weight, plus the component of F acting in the Y-direction, along with a reasonable value for the static friction coefficient between the boulder and the ground will result in a large friction force, f_1, that will tend to prevent sliding of the boulder. In addition, for an impact velocity of 2000 fps, the time of contact between the boulder and the EPW will be on the order of 1 ms, which is too short a time for a 4-foot diameter boulder to respond as a rigid body. It is quite possible, of course, that a complete analysis of some other impact conditions will require an appropriate treatment of the boulder's motion. However, since it is expected that such analyses will be quite complex, they will be reserved for a separate, future study.

As a final simplification, we assume that the friction force between the EPW and the boulder, f_2, is zero. This assumption is justified by empirical studies indicating that the coefficient of sliding friction between a rock and a metal surface is on the order of 0.08 at high relative velocities [7].

It should also be noted that a special situation exists when the contact angle, θ, is less than $90 - \gamma + \phi$. When this condition occurs, the EPW's nose tip will not contact

the boulder. The contact area and the loading duration will be reduced, consequently reducing the lateral impulse. One scenario to illustrate this situation is given by an EPW with an initial impact angle of 90 degrees striking a spherical boulder as in Figure 5; the limiting contact angle would be ϕ, the nose cone angle (about 12 to 20 degrees). There is no such limitation for impacts with planar obstacles (e.g. a concrete slab).

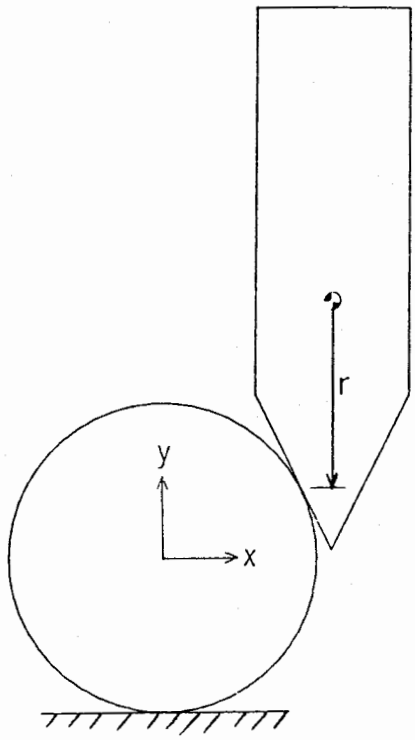

Figure 5. Effect of Reduced Moment Arm and Lateral Load Due to a Smaller Area of Contact.

2.2. Solving for the Impact Angle, γ

An expression for the final impact angle, γ_3, was derived first since it is independent of the other angles. The value of the impact angle at Point 2 can be computed by assuming the lateral impulse produces a constant angular acceleration:

$$\gamma_2 = \gamma_1 + \dot{\gamma}_1 t_{12} + \frac{1}{2}\ddot{\gamma}_{12} t_{12}^2, \tag{1}$$

where, in this case, positive γ is taken as counterclockwise, and

$$t_{12} = \frac{L_n}{v_1}, \tag{2}$$

$\dot{\gamma}_1$ is the first time derivative of the impact angle at Point 1, and $\ddot{\gamma}_{12}$ is the second derivative of the impact angle during time t_{12}. A similar equation can represent the change in γ from Point 2 to Point 3 where only gravity acts as a linear acceleration; furthermore, the angular velocity, $\dot{\gamma}_2$, is not zero. Thus an expression for γ_3 is given by:

$$\gamma_3 = \gamma_2 + \dot{\gamma}_2 t_{23} + \frac{1}{2}\ddot{\gamma}_{23} t_{23}^2 \tag{3}$$

where t_{23} is the time from Point 2 to Point 3, $\dot{\gamma}_2$ is the first time derivative of the impact angle at Point 2, and $\ddot{\gamma}_{23}$ is the second time derivative during the time t_{23} and is assumed to be zero since there are no external forces acting on the penetrator during this time. Substituting (1) into (2) we get

$$\gamma_3 = \gamma_1 + \dot{\gamma}_1 t_{12} + \frac{1}{2}\ddot{\gamma}_{12} t_{12}^2 + \dot{\gamma}_2 t_{23}. \tag{4}$$

The angular velocity, $\dot{\gamma}_2$, can be calculated at Point 2 from the equation

$$\dot{\gamma}_2 = \dot{\gamma}_1 + \ddot{\gamma}_{12} t_{12}. \tag{5}$$

We now solve for the angular acceleration from the moment equation, where F is a constant lateral force (assumed to act normal to the contacting tangential plane), and r is the distance from the tip of the penetrator's nose to its center of gravity. Thus:

$$\sum M_{cg} = \ddot{\gamma}_{12} I_{cg} \rightarrow \ddot{\gamma}_{12} = -\frac{Fr}{I_{cg}} \sin(\gamma_1 + \theta) \tag{6}$$

where I_{cg} is the pitch moment of inertia of the penetrator, and θ is the contact angle. We substitute (6) into (5), and subsequently substitute (5) into (4); This resolves into

$$\gamma_3 = \gamma_1 + \dot{\gamma}_1 \left[t_{23} + t_{12}\right] - \frac{Fr}{I_{cg}} \sin(\gamma_1 + \theta) \left[t_{12}^2 + t_{12} t_{23}\right]. \tag{7}$$

But t_{23} is still unknown; this can be solved from the quadratic equation which is derived from Newton's Second Law in the vertical direction. Thus:

$$t_{23}^2 - \frac{2}{g}\left[-v_1 \sin(\alpha_1 + \gamma_1) + \frac{F t_{12}}{M} \sin(\theta)\right] t_{23} - \frac{2}{g} y_2 = 0 \tag{8}$$

where M is the mass of the penetrator, and y_2 is the distance from Point 2 to the ground. If the gravity term is negligible after the projectile leaves the object, then

$$t_{23} = \frac{y_2}{v_1 \sin(\alpha_1 + \gamma_1) + F \frac{t_{12}}{M} \sin(\theta)}. \tag{9}$$

Using this equation for t_{23} for the EPW calculations amounted to less than 1% difference. y_2 is also unknown but can be evaluated from:

$$y_2 = H - v_1 \sin(\alpha_1 + \gamma_1) t_{12} - \frac{1}{2}\left[\ddot{y}_2 - \frac{F}{M} \sin(\theta)\right] t_{12}^2, \tag{10}$$

where

$$H = \frac{D}{2}\left[1 + \sin(\theta)\right] \tag{11}$$

in the case of a spherical boulder. The time rate of change in the unit vector of the velocity term is

$$\ddot{y}_2 = v_1(\dot{\gamma}_1 + \dot{\alpha}_1)\cos(\alpha_1 + \gamma_1). \tag{12}$$

Since $\dot{\gamma}_1$ and $\dot{\alpha}_1$ were assumed to be zero, $\ddot{y}_2$ is also zero. The change in the magnitude of the velocity results from the axial component of the force.

3.1. Initial Angle of Attack, α_1

DOD
MCTL
(3)

DOD
MCTL
(3)

3.4. Height at Point of Contact, H

3.5. Force Between the Boulder and the Penetrator, F

DOD
MCTL
(3)

b(3)

DOD
NCTL
b(3)

DOD
MCTL
b(3)

DOD
MCTL
b(3)

DOD
MCTL
b(3)

3.8. Summary

DOD
MCTL
b(3)

DOD
NTL
b3

DOD
NCTL
b(3)

DOD
MCTL
V13

DOD
MCTL
b(3)

DCD
MCIL
b(5)

DOD
MCTL
b(3)

DOD
MCTL
b(3)

DOD
MCTL
b(3)

References

1. R. B. Nelson, Y. M. Ito, D. E. Burks, Y. Muki, J. A. Hollowell, and C. W. Miller, "Numerical Analysis of Projectile Penetration Into Boulder Screens," SL-83-11, U.S. Army Waterways Experiment Station, July 1983.

2. C. W. Miller, W. L. McKay, and J. A. Hollowell, "Penetration of $\frac{1}{7}$ Scale Model of a Semi–Armor Piercing (SAP) Bomb Into Confined Overlays: Test and Analysis," AVCO Systems Div., SL-83-19, U.S. Army Waterways Experiment Station, Sept. 1983.

3. Y. M. Ito, R. B. Nelson, and D. E. Burks, "Numerical Method for Rock Rubble Fortification Analysis," DNA 5869F, Cal Research and Tech., July 1981.

4. C. F. Austin, C. C. Halsey, and S. L. Berry, "Full–Scale Penetration Into Semi-confined Diorite Boulders by a Semi-Armor Piercing (SAP) Bomb and a Slendor Penetrator," NWCTP 6220, Naval Weapons Center, Sept. 1980.

5. D. A. Matuska and J.J. Osborn, HULL Documentation, VOL 1 (Technical Manual) and VOL 2 (Users Manual), Orlando Technology Report, Shalimar, Florida, 1987.

6. Y. M. Ito, R. B. Nelson, and F. W. Ross–Perry, "3–D Numerical Analyses of Earth Penetrator Dynamics," DNA 5404F, Defense Nuclear Agency, Jan 1979.

7. M. M. Hightower, private communication.

8. P. Yarrington, private communication.

9. M. L. Chiesa, private communication.

INITIAL DISTRIBUTION

EXPORT CONTROLLED INFORMATION

R. W. Taylor, LANL, NWAP/MS F634
J. L. Kammerdiener, LANL, NWAP/MS F634
H. R. Lehman, LANL, WP/MS F631

H. W. Kruger, LLNL, L-84
J. O'dell, LLNL, L-85
R. F. Perret, LLNL, L-81
R. D. Streit, LLNL, L-125
H. C. Vantine, LLNL, L-35

1533	P. Yarrington
5160	G. R. Otey
5161	K. D. Nokes
5161	A. B. Cox
5115	S. D. Meyer
5111	W. J. Patterson
8000	J. C. Crawford
	Attn: E. E. Ives, 8100
	R. J. Detry, 8200
	P. L. Mattern, 8300
	R. C. Wayne, 8400
	P. L. Brewer, 8500
8150	J. B. Wright
8171	C. B. Layne
8171	R. N. Everett
8171	C. T. Oien
8154	D. J. Havlik
8156	M. F. Horstemeyer (10)
8240	C. W. Robinson
8241	G. A. Benedetti
8241	M. L. Chiesa
8310	R. W. Rohde
8316	J. B. Woodard
8316	J. Lipkin (5)
8430	J. Vitko
8436	N. A. Lapetina
8436	J. C. Swearengen
9122	M. M. Hightower
9122	C. W. Young

8535	Publications for OSTI (2)
8535	Publications/Technical Library Processes, 3141
3141	Technical Library Processes Division (3)
8524-2	General Technical Files (3)

NORDA
Polar Oceanography Branch
72 Lyme Road
Hanover, NH 03755
  For: James P. Welsh

USA CRREL (4)
72 Lyme Road
Hanover, NH 03755
  For: David Cole
       Gordon Cox
       J. Richter-Menge
       Terry Tucker

Naval Polar Ocean Center
4301 Suitland Road
Washington, DC 20390
  For: Donald Barnett

Analysis and Technology
2121 Crystal Drive, Suite 800
Arlington, VA 22202
  For: George Newton

Science Applications International Corp.
205 Montecito Avenue
Monterey, CA 93940
  For: Warren W. Denner

Greenridge Sciences, Inc.
5276 Hollister Ave, Suite 408
Santa Barbara, CA 93111
  For: Charles R. Greene

Pacifica Technology
P. O. Box 148
Del Mar, CA 92014
  For: Robert T. Allen

AT&T Bell Laboratories
Whippany Road
Whippany, NJ 07981.
   For: Mr. R. B. Stratton

Matrix Corp.
8150 Leesburg Pike, Suite 1000
Vienna, VA 22180
  For: Robert Parris

Naval Intelligence Support Center
4301 Suitland Rd.
Washington, D. C. 20390-5140
  For: Peter L. Findlay

Naval Underwater System Center
New London Lab.
New London, CT 06320
  For: Robert Greenlaw

Sippican Inc.
Barnabas Road
Marion, MA 02738
  For: Richard Bixby

Sparton Electronics Corporation
1215 Jefferson Davis Hwy.
Arlington, VA 22202
  For: Robert Miller

Geophysical Institute
University of Alaska
Fairbanks, AL 99775-0800
  For: Prof. William Sackinger

General Dynamics, Pomona Division
1675 W. Mission Blvd.
P. O. Box 2507
Pomona, CA 91769-2507
  For: John McElwee

Polar Research Lab
6308 Carpinteria Ave
Carpinteria, CA 93013
  For: Bo Buck

National Data Buoy Cntr
NSTL, MS 39529
  For: Phil Kies

Arctic Analysts, Inc.
P. O. Box 2149
Boulder, CO 80306
  For: Capt. Alfred S. McLaren USN (ret)

University of Washington
Applied Physics Laboratory
Seattle, WA 98105
  For: Robert E. Francois

R. G. Couch, LLNL, L-6
S. A. Erickson, LLNL, L-83
D. E. Magnoli, LLNL, L-83
W. B. Shuler, LLNL, L-6

Larkin Garcia, LANL MSF601

0400 J. C. Swearengen
1533 P. Yarrington
1533 G. I. Kerley
5110 C. C. Burks
5112 R. R. Beasley
5161 K. D. Nokes
5120 W. R. Reynolds
7170 R. D. Bentley
7530 T. B. Lane
7531 D. R. Schafer
8000 J. C. Crawford; Attn: R. J. Detry, 8200
P. L. Mattern, 8300
P. E. Brewer, 8500
8100 E. E. Ives; Attn: L. A. Hiles, 8130
J. F. Barham, 8140
D. J. Bohrer, 8160
R. A. Baroody, 8180
8100-A R. L. Rinne
8131 W. R. Bolton
8133 A. C. Skinrood; Attn: 8133 E. H. Carrell
8133 L. G. Radosevich
8142 M. A. Gusinow; Attn: 8142 H. D. Sorensen
8142 D. C. Stoner
8150 J. B. Wright; Attn: 8154 D. J. Havlik
8155 J. B. Woodard
8165 S. G. Cain
8170 J. W. Hickman
8171 C. B. Layne
8171 R. N. Everett
8171 C. T. Oien
8171 G. E. Strandin
8172 R. B. Gallagher
8173 M. E. John; Attn: J. P. Hinton
8240 C. B. Robinson; Attn: 8241 B. A. Benedetti
8241 M. L. Chiesa
8357 R. W. Carling
8400 R. C. Wayne; Attn: H. Hanser, 8440
J. F. Barham, 8450
8430 J. Vitko
8431 L. A. West
8432 M. Hall
8432 J. S. Kraabel
8435 D. W. Sweeney
8436 M. T. Ferrario
8436 R. E. Rychnovsky (10)
9000 R. L. Hagengruber; Attn: W. C. Hines 9010
9011 G. S. Brown; Attn: R. L. Woodfin
J. F. Arfman
9100 R. G. Clem
9121 L. T. James
9122 R. H. Braasch
9122 C. J. Northrup
9122 C. W. Young

8535 Publications Division for OSTI (2)
8535 Publications/Technical Library Processes, 3141
3141 Technical Library Processes Division (3)
8524 P. W. Dean for Central Technical Files (3)